Національна академія наук України

ІНСТИТУТ
ФІЗИКИ
КОНДЕНСОВАНИХ
СИСТЕМ

ICMP–16–08E

Vasyl Baliha, Johannes Richter,* Oleg Derzhko

ONE-DIMENSIONAL TASAKI-HUBBARD MODEL
IN PARAMAGNETIC LIMIT

*Institut für theoretische Physik, Otto-von-Guericke-Universität Magdeburg, P.O. Box 4120, 39016 Magdeburg, Germany

ЛЬВІВ

Одновимірна модель Тасакі-Габарда у парамагнітній границі

В. Баліга, Й. Ріхтер, О. Держко

Анотація. Одновимірна модель Тасакі-Габарда належить до класу плоскозонних феромагнетиків. Ввівши безмежно мале зовнішнє магнітне поле, ми досліджуємо властивості цієї моделі у парамагнітному режимі. Ми порівнюємо і співставляємо ці властивості з властивостями звичайного парамагнетика Кюрі.

One-dimensional Tasaki-Hubbard model in paramagnetic limit

V. Baliha, J. Richter, O. Derzhko

Abstract. The one-dimensional Tasaki-Hubbard model belongs to the class of flat-band ferromagnets. By introducing an infinitesimally small external magnetic field, we examine the properties of the model in the paramagnetic regime. We compare and contrast them to the properties of the conventional Curie paramagnet.

Василь Ярославович Баліга
Йоганнес Ріхтер
Олег Володимирович Держко

Одновимірна модель Тасакі-Габарда у парамагнітній границі

1. Introduction

In 1992 H. Tasaki considered the standard (repulsive) one-orbital Hubbard model with the Hamiltonian

$$H = \sum_{\sigma=\uparrow,\downarrow} H_{0,\sigma} + H_U,$$

$$H_{0,\sigma} = \sum_{(ij)} t_{ij} \left(c_{i,\sigma}^\dagger c_{j,\sigma} + c_{j,\sigma}^\dagger c_{i,\sigma} \right), \quad t_{ij} > 0,$$

$$H_U = U \sum_i n_{i,\uparrow} n_{i,\downarrow}, \quad U > 0 \tag{1.1}$$

on the so-called decorated lattices which support a completely dispersionless (flat) lowest-energy one-electron band [1]. In one dimension the introduced lattice is also known as the sawtooth chain or the Δ-chain with a special relation between the hopping integrals along the straight line t_1 and the zigzag path t_2: $t_2 = \sqrt{2}t_1 > 0$, see Fig. 1. It is well known [1] that the ground state of the model is the fully polarized (i.e., saturated) ferromagnetic state, i.e., $\langle \mathbf{S}^2 \rangle_{n,\mathcal{N}} = (n/2)[(n/2) + 1]$, if the number of electrons n equals $\mathcal{N} = N/2$ or $\mathcal{N} - 1$. For smaller numbers of electrons, $1 < n < \mathcal{N} - 1$, we have $0 < \langle \mathbf{S}^2 \rangle_{n,\mathcal{N}} < (n/2)[(n/2) + 1]$ (nonsaturated ferromagnetism). Furthermore, $\lim_{N\to\infty} \langle \mathbf{S}^2 \rangle_{n,\mathcal{N}}/n^2 = 0$, if $n/N < 1/2$. In other words, thermodynamically large systems exhibit ground-state ferromagnetism for $n/N = 1/2$ but are paramagnetic for $0 < n/N < 1/2$.
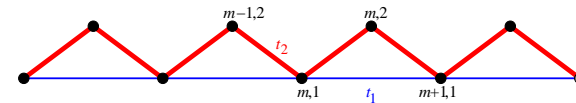

Figure 1. (Color online) One-dimensional Tasaki lattice. Here $t_2 = \sqrt{2}t_1 > 0$.

The Mielke-Tasaki mechanism for the ground-state ferromagnetism can be explained as follows [1–5]. $\mathcal{N}$ states from the lowest-energy flat band with the energy $\varepsilon_1 = -2t_1$ can be visualized as localized within a V-shaped part of the chain (trapping cell), i.e., the flat-band states are given by $l_{m,\sigma}^\dagger |0\rangle$, $l_{m,\sigma}^\dagger = c_{m-1,2,\sigma}^\dagger - \sqrt{2}c_{m,1,\sigma}^\dagger + c_{m,2,\sigma}^\dagger$, $m = 1, \ldots, \mathcal{N}$, see Fig. 1. Neighboring traps have common sites (the sites $m,2$, $m = 1, \ldots, \mathcal{N}$, see Fig. 1). The ground states for $1 < n < \mathcal{N} - 1$ electrons consist of sets of independent clusters, where each cluster is built by connected occupied

traps with electrons in the symmetric spin state (ferromagnetic cluster). The many-electron ground-state states of H (1.1) constructed this way do not feel the Hubbard repulsion $U > 0$ and belong at the same time to the ground-state manifold of the noninteracting system with the energy $n\varepsilon_1$. For $n = \mathcal{N}$ and $n = \mathcal{N} - 1$ no isolated clusters exist, i.e., only a single ferromagnetic cluster can be constructed. Therefore the ground state is ferromagnetic with the maximal value of $\langle \mathbf{S}^2 \rangle_{n,\mathcal{N}}$. For smaller $1 < n < \mathcal{N} - 1$ isolated clusters can appear and $\langle \mathbf{S}^2 \rangle_{n,\mathcal{N}}$ is less than its maximal value $\mathbf{S}_{\max}^2 = (n/2)[(n/2) + 1]$.

Furthermore, one can calculate the number of the ground states, i.e., the ground-state degeneracy [5–7]. By mapping the ground states of $n < \mathcal{N}$ electrons of the N-site Tasaki chain onto the spatial configurations of n hard dimers on a $2\mathcal{N}$-site simple chain [6] one can find the ground-state degeneracy $g_{\mathcal{N}}(n)$:

$$g_{\mathcal{N}}(n) = \frac{2\mathcal{N}}{2\mathcal{N} - n} \mathcal{C}_{2\mathcal{N}-n}^n. \tag{1.2}$$

Bearing in mind that the canonical partition function of n electrons on the Tasaki chain of volume $\mathcal{N} = N/2$ cells is $Z(T, n, \mathcal{N}) = g_{\mathcal{N}}(n)e^{-n\varepsilon_1/T}$, we immediately get from Eq. (1.2) the Helmholtz free energy $F(T, n, \mathcal{N}) = -T \ln Z(T, n, \mathcal{N})$,

$$F(T, n, \mathcal{N}) = -\mathcal{N}T \ln \frac{(2-p)^{2-p}}{p^p(2-2p)^{2-2p}} + n\varepsilon_1, \tag{1.3}$$

where $p = n/\mathcal{N}$ is the electron density. Alternatively, one can calculate the grand-canonical partition function [6, 7]

$$\Xi(T, \mu, \mathcal{N}) = \left(\frac{1}{2} + \sqrt{\frac{1}{4} + e^{\frac{\mu - \varepsilon_1}{T}}} \right)^{2\mathcal{N}} \tag{1.4}$$

and the grand thermodynamical potential

$$\Omega(T, \mu, \mathcal{N}) = -2\mathcal{N}T \ln \left(\frac{1}{2} + \sqrt{\frac{1}{4} + e^{\frac{\mu - \varepsilon_1}{T}}} \right). \tag{1.5}$$

The thermodynamic functions in Eq. (1.3) and Eq. (1.5) are related by the Legendre transformation $F = \Omega + \mu n$ after eliminating μ in the r.h.s. of this equation using the relation $n = -\partial\Omega/\partial\mu$. Formulas (1.3) or (1.5) give the contribution of the highly degenerate ground-state manifold to thermodynamics of the considered Hubbard model. This contribution

dominates for $0 \le p \le 1$ or for $\mu \approx \varepsilon_1$ in the low-temperature regime [5–7].

In the present paper, we wish to extend the previous investigations [6, 7] switching on an infinitesimally small external magnetic field $h > 0$ [8], i.e., the field is nonzero but it presents the smallest energy scale in the problem. We are interested in the case $1 \le n < \mathcal{N} - 1$, that is the case which yields paramagnetism in the thermodynamic limit $n \to \infty$, $\mathcal{N} \to \infty$, $0 < p = n/\mathcal{N} < 1$. Our aim is to study the peculiarities of the one-dimensional Tasaki-Hubbard paramagnet compared to the conventional spin-1/2 Curie paramagnet. These peculiarities arise (i) from the degeneracy of the ground-state manifold, (ii) from the larger size of the individual magnetic moments (which are proportional to the size of the isolated ferromagnetic clusters), and (iii) from the distribution of the size of the ferromagnetic clusters. For completeness, we give here the Helmholtz free energy of the spin-1/2 Curie paramagnet

$$f_{\mathrm{C}}(T, h) = -T \ln \frac{\sinh \frac{h}{T}}{\sinh \frac{h}{2T}} = -T \ln \left(2 \cosh \frac{h}{2T} \right). \tag{1.6}$$

To this end, we consider finite chains consisting of $N = 12$, 16, 20, 24 sites. After characterizing the ground-state manifold for various numbers of electrons $n = 1, \ldots, N/2$, we calculate the canonical partition functions and thermodynamic quantities. We compare the results with the case $h = 0$, discuss the $1/N \to 0$ limit, and contrast the results for the Tasaki-Hubbard and Curie paramagnets. The discussion of finite chains allows also to check the obtained analytical results (obtained by taking into account only the flat-band cluster states) by comparing them with exact-diagonalization data for the full Hubbard model (i.e., taking into account all eigenstates) for chains of $N = 16$ sites (finite U) and $N = 24$ sites ($U \to \infty$).

2. Results

In what follows we consider the canonical description for finite chains with $\mathcal{N} = 6$, 8, 10, 12 trapping cells. Note that in previous papers [5–7] on model (1.1) the focus was on grand-canonical description. In the presence of magnetic field the formula for $Z(T, n, \mathcal{N})$ must be modified. Consider, for example, the case $n = 4$ and $\mathcal{N} = 6$. According to Eq. (1.2) for $h = 0$ we get $g_6(4) = 105$, and therefore $Z(T, 4, 6) = 105e^{-4\varepsilon_1/T}$. The ground-state degeneracy 105 comes from 6 spatial single-cluster configurations (each spatial configuration has degeneracy 5), 6 spatial
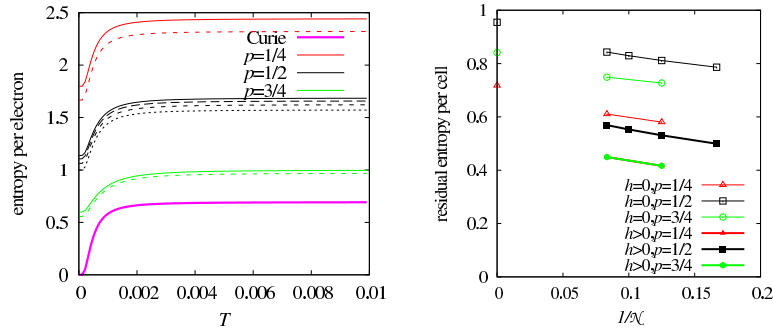
Figure 2. (Color online) Left panel: Temperature dependence of the entropy per electron $s(T, h, p)$ for $h = 0.001$ and $p = 1/4$ (red), $p = 1/2$ (black), and $p = 3/4$ (green). The results for $\mathcal{N} = 6$, 8, 10, 12 cells are shown by dotted, short-dashed, long-dashed, solid curves, respectively. The bold magenta curve corresponds to the Curie paramagnet. Right panel: Dependence of the residual entropy per cell $S(T = 0, h, n, \mathcal{N})/\mathcal{N}$ on $1/\mathcal{N}$ for $h = 0$ (thin curves) and $h > 0$ (thick curves) for electron concentrations $p = 1/4$ (red), $p = 1/2$ (black), and $p = 3/4$ (green). Note that the thick red and green curves coincide. The results in the thermodynamic limit for $h = 0$ are shown by symbols on the ordinate axis (i.e., at $1/\mathcal{N} = 0$).

configurations "3-site cluster + 1-site cluster" (each spatial configuration has degeneracy 8), and 3 spatial configurations "2-site cluster + 2-site cluster" (each spatial configuration has degeneracy 9). If $h > 0$ the mentioned states have different energies resulting in the new formula for $Z(T, h, 4, 6)$:

$$Z(T, h, 4, 6) = e^{-\frac{4\varepsilon_1}{T}}$$
$$\times \left[6 \left(e^{\frac{2h}{T}} + e^{\frac{h}{T}} + 1 + e^{-\frac{h}{T}} + e^{-\frac{2h}{T}} \right) \right.$$
$$+ 6 \left(e^{\frac{3h}{2T}} + e^{\frac{h}{2T}} + e^{-\frac{h}{2T}} + e^{-\frac{3h}{2T}} \right) \left(e^{\frac{h}{2T}} + e^{-\frac{h}{2T}} \right)$$
$$\left. + 3 \left(e^{\frac{h}{T}} + 1 + e^{-\frac{h}{T}} \right)^2 \right]. \qquad (2.1)$$

The calculation of the Helmholtz free energy per electron $f_{\mathrm{TH}}(T, h, p) = -T \ln Z(T, h, n, \mathcal{N})/n$ and of other thermodynamic quantities is straightforward now and can be done using a software for analytical calculations.
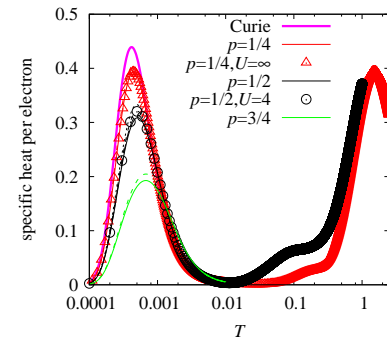

Figure 3. (Color online) Temperature dependence of the specific heat per electron $c(T, h, p)$ for $h = 0.001$ and $p = 1/4$ (red), $p = 1/2$ (black), and $p = 3/4$ (green). The results for $\mathcal{N} = 6$, 8, 10, 12 cells are shown by dotted, short-dashed, long-dashed, solid curves, respectively. The bold magenta curve corresponds to the Curie paramagnet. By symbols we show exact-diagonalization data for the Hubbard model (1.1) with $U = 4$, $N = 16$, $n = 4$ (circles) and $U \to \infty$, $N = 24$, $n = 3$ (triangles).
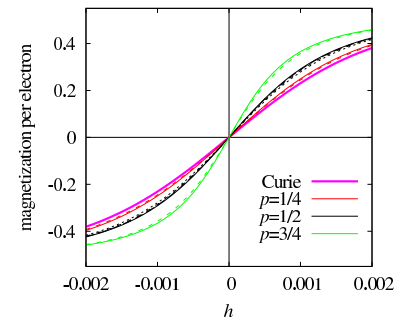

Figure 4. (Color online) Field dependence of the magnetization per electron $m(T, h, p)$ for $T = 0.001$ and $p = 1/4$ (red), $p = 1/2$ (black), and $p = 3/4$ (green). The results for $\mathcal{N} = 6$, 8, 10, 12 cells are shown by dotted, short-dashed, long-dashed, solid curves, respectively. The bold magenta curve corresponds to the Curie paramagnet.

Figure 5. (Color online) Temperature dependence of the susceptibility per electron $\chi(T, h, p)$ multiplied by T for $h = 0$ and $p = 1/4$ (red), $p = 1/2$ (black), and $p = 3/4$ (green). The results for $\mathcal{N} = 6, 8, 10, 12$ cells are shown by dotted, short-dashed, long-dashed, solid curves, respectively. T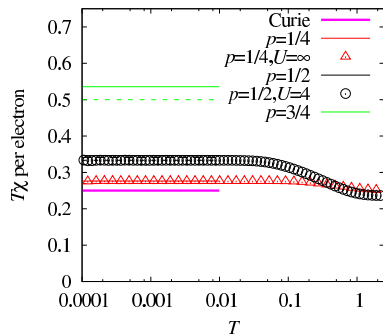he bold magenta curve corresponds to the Curie paramagnet. By symbols we show exact-diagonalization data for the Hubbard model (1.1) with $U = 4$, $N = 16$, $n = 4$ (circles) and $U \to \infty$, $N = 24$, $n = 3$ (triangles).

Our results are reported in Figs. 2 – 6. The temperature dependence of the entropy and of the specific heat are presented in Figs. 2 and 3, respectively. For zero field, $h = 0$, we know [5–7] that the huge ground-state degeneracy leads to a nonzero residual entropy, i.e., $S(T, h = 0, n, \mathcal{N})/n = [\ln g_{\mathcal{N}}(n)]/n \neq 0$, as well as a vanishing specific heat, i.e., $C(T, h = 0, n, \mathcal{N}) = 0$. By switching on h the degeneracy of the ground-state manifold is partly lifted, however, the degeneracy remains huge such that a nonzero residual entropy (although reduced) survives, see Fig. 2. Trivially, for the ordinary Curie paramagnet the ground state at $h > 0$ is the single ferromagnetic state, i.e., there is no residual entropy. The finite-size dependence sketched in the right panel of Fig. 2 gives evidence that the residual entropy is present for $N \to \infty$.

The specific heat at nonzero h shows already a nontrivial dependence on temperature and agrees with exact-diagonalization data for model (1.1) at low temperatures, see Fig. 3. Moreover, finite size-effects are small (results for $\mathcal{N} = 6, 8, 10, 12$ almost coincide). As p increases, deviations from the Curie-paramagnet case become more pronounced (peak becomes lower and broader) and $C(T, h, n, \mathcal{N}) \to 0$, when $p \to 1$. That indicates that less excited states are accessible in the Tasaki-Hubbard system.

The low-temperature magnetization curves in Fig. 4 show that it is easier to magnetize the Tasaki-Hubbard paramagnet with $p > 0$ than the Curie paramagnet, i.e., Tasaki-Hubbard paramagnet shares properties with a superparamagnet. This is in agreement with results for the initial (zero-field) susceptibility shown in Fig. 5.

Finally, we discuss the ground-state magnetic properties of the Tasaki-Hubbard paramagnet at $h = 0$. To this end, we calculate the average square of the total spin $\langle \mathbf{S}^2 \rangle_{n,\mathcal{N}}$ [7,9]. The direct way to get $\langle \mathbf{S}^2 \rangle_{n,\mathcal{N}}$ is to use its definition. For the considered example $n = 4$, $\mathcal{N} = 6$, in 30 states $\mathbf{S}^2$ has the value 6, in 48 states $\mathbf{S}^2$ has the value $9/2$, and in 27 states $\mathbf{S}^2$ has the value 4. Therefore $\langle \mathbf{S}^2 \rangle_{4,6} = 24/5$. An alternative way to get $\langle \mathbf{S}^2 \rangle_{n,\mathcal{N}}$ is to calculate first the (normalized) number of clusters with l electrons, $n(l)$, and then to sum up $\sum_{l=1}^{n} n(l)(l/2)[(l/2)+1]$, see Ref. [9]. For the considered example, $n(1) = 48/105$, $n(2) = 54/105$, $n(3) = 48/105$, and $n(4) = 30/105$ resulting again in $\langle \mathbf{S}^2 \rangle_{4,6} = 24/5$. The latter approach is convenient in the percolation setup, since the cluster-size distribution $n(l)$ can be obtained either analytically or numerically. Thus, in the one-dimensional case, $\langle \mathbf{S}^2 \rangle_{n,\mathcal{N}}/\mathcal{N} = 3p(2 - p)/[8(1 - p)]$ in the thermodynamic limit [9]. A third possibility to get $\langle \mathbf{S}^2 \rangle_{n,\mathcal{N}}$ is to exploit the Curie law for the temperature dependence of the initial susceptibility, $\chi(T, h = 0) = C/T$, since for Curie constant holds $C = \langle \mathbf{S}^2 \rangle_{n,\mathcal{N}}/3$. Using the latter approach we arrive at

$$\langle \mathbf{S}^2 \rangle_{n,\mathcal{N}} = 3T^2 \frac{\partial^2 \ln Z(T, h, n, \mathcal{N})}{\partial h^2}\bigg|_{h=0}. \qquad (2.2)$$

In Table 1 we collect our findings for $\langle \mathbf{S}^2 \rangle_{n,\mathcal{N}}$, $n = 1, \ldots, \mathcal{N} - 1$ which coincide with the ones for $\mathcal{N} = 6, 8$ presented earlier in Ref. [7]. In Fig. 6 we show the results for $\langle \mathbf{S}^2 \rangle_{n,\mathcal{N}}$ obtained by Eq. (2.2) demonstrating that (i) ferromagnetism disappears for $0 < p < 1$ as $\mathcal{N}$ increases (main panel) and (ii) $\langle \mathbf{S}^2 \rangle_{n,\mathcal{N}}/\mathcal{N}$ approaches $3p(2-p)/[8(1-p)]$ (bold black curve) [9] as $\mathcal{N}$ increases (inset).

3. Conclusions

To summarize, in the present study we have extended the analysis of Refs. [6, 7] for the Tasaki-Hubbard chain: We switch on an infinitesimally small external magnetic field and show how previous findings become modified. At small electron densities the system is a paramagnet. However, it differs from the conventional Curie paramagnet, rather it resembles a superparamagnet with a huge degeneracy of the ground state and a size-distribution the ferromagnetic clusters. Comparison to
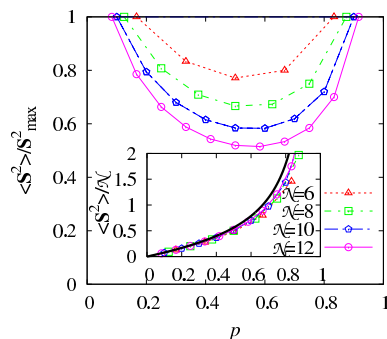
Figure 6. (Color online) Main panel: Dependence of the averaged (over ground states) total spin squared $\langle \mathbf{S}^2 \rangle_{n,\mathcal{N}}$ per its maximal value $\mathbf{S}^2_{\max} = (n/2)[(n/2)+1]$ on the electron density p. The results for $\mathcal{N} = 6, 8, 10, 12$ cells are shown by dotted, short-dashed, long-dashed, solid curves, respectively. Inset: Dependence of the averaged (over ground states) total spin squared $\langle \mathbf{S}^2 \rangle_{n,\mathcal{N}}$ per cell on the electron density p. The bold black curve corresponds to the $\mathcal{N} \to \infty$ result obtained in Ref. [9], see the main text of the paper.

Table 1. Values of $\langle \mathbf{S}^2 \rangle_{n,\mathcal{N}}$ for Tasaki chains with different number of electrons and cells as they follow from Eq. (2.2).

n	1	2	3	4	5	6	7	8	9	10	11
$\mathcal{N} = 6$	$\frac{3}{4}$	$\frac{5}{3}$	$\frac{81}{28}$	$\frac{24}{5}$	$\frac{35}{4}$						
$\mathcal{N} = 8$	$\frac{3}{4}$	$\frac{21}{13}$	$\frac{117}{44}$	4	$\frac{165}{28}$	9	$\frac{63}{4}$				
$\mathcal{N} = 10$	$\frac{3}{4}$	$\frac{27}{17}$	$\frac{51}{20}$	$\frac{48}{13}$	$\frac{225}{44}$	7	$\frac{39}{4}$	$\frac{72}{5}$	$\frac{99}{4}$		
$\mathcal{N} = 12$	$\frac{3}{4}$	$\frac{11}{7}$	$\frac{189}{76}$	$\frac{60}{17}$	$\frac{19}{4}$	$\frac{81}{13}$	$\frac{357}{44}$	$\frac{32}{3}$	$\frac{405}{28}$	21	$\frac{143}{4}$

exact-diagonalization data shows that the elaborated approach is appropriate for description of the low-temperature properties of the Tasaki-Hubbard-chain paramagnet. While with modest efforts the calculation of $Z(T, h, n, \mathcal{N})$ can be extended for larger $\mathcal{N}$, exact-diagonalization computations for $n = 6$ ($n = 5$) electrons and $\mathcal{N} = 8$ ($\mathcal{N} = 12$) cells if U is finite (if $U \to \infty$) are at the nowadays limits.

Acknowledgments

References

1. H. Tasaki, Phys. Rev. Lett. **69**, 1608 (1992).
2. A. Mielke, J. Phys. A **24**, L73 (1991); A. Mielke, J. Phys. A **24**, 3311 (1991); A. Mielke, J. Phys. A **25**, 4335 (1992); A. Mielke, Phys. Lett. A **174**, 443 (1993).
3. A. Mielke and H. Tasaki, Commun. Math. Phys. **158**, 341 (1993).
4. H. Tasaki, J. Phys.: Condens. Matter **10**, 4353 (1998); H. Tasaki, Prog. Theor. Phys. **99**, 489 (1998).
5. O. Derzhko, J. Richter, and M. Maksymenko, Int. J. Mod. Phys. B **29**, 1530007 (2015).
6. O. Derzhko, A. Honecker, and J. Richter, Phys. Rev. B **76**, 220402(R) (2007).
7. O. Derzhko, J. Richter, A. Honecker, M. Maksymenko, and R. Moessner, Phys. Rev. B **81**, 014421 (2010).
8. Here $h = g\mu_B \mathsf{H}$, where H is the magnetic field measured in Tesla, $\mu_B \approx 0.67171 \mathrm{K/T}$ is the Bohr magneton, and g is the electron g-factor.
9. M. Maksymenko, A. Honecker, R. Moessner, J. Richter, and O. Derzhko, Phys. Rev. Lett. **109**, 096404 (2012).